High-precision mass measurement of neutron-rich 96Kr

Matthew B. Smith, Tobias Murböck, Eleanor Dunling, Andrew Jacobs, Brian Kootte, Yang Lan, Erich Leistenschneider, David Lunney, Eleni Marina Lykiardopoulou, Ish Mukul, et al.

High-precision mass measurement of neutron-rich 96Kr

Matthew B. Smith · Tobias Murböck · Eleanor Dunling · Andrew Jacobs · Brian Kootte · Yang Lan · Erich Leistenschneider · David Lunney · Eleni Marina Lykiardopoulou · Ish Mukul · Stefan F. Paul · Moritz P. Reiter · Christian Will · Jens Dilling · Anna A. Kwiatkowski

Received: date / Accepted: date

Matthew B. Smith · Tobias Murböck · Eleanor Dunling · Andrew Jacobs · Brian Kootte · Yang Lan · Erich Leistenschneider · Eleni Marina Lykiardopoulou · Ish Mukul · Stefan F. Paul · Moritz P. Reiter · Jens Dilling · Anna A. Kwiatkowski
TRIUMF, 4004 Wesbrook Mall, Vancouver, BC V6T 2A3, Canada

Eleanor Dunling
Department of Physics, University of York, York YO10 5DD, United Kingdom

Andrew Jacobs · Yang Lan · Erich Leistenschneider · Eleni Marina Lykiardopoulou · Jens Dilling
Department of Physics and Astronomy, University of British Columbia, Vancouver, British Columbia V6T 1Z1, Canada

Brian Kootte
Department of Physics and Astronomy, University of Manitoba, Winnipeg, Manitoba R3T 2N2, Canada

David Lunney
CSNSM-IN2P3, Université de Paris Sud, Orsay, France

Stefan F. Paul
Ruprecht-Karls-Universität Heidelberg, D-69117 Heidelberg, Germany

Moritz P. Reiter · Christian Will
II. Physikalisches Institut, Justus-Liebig-Universität, 35392 Gießen, Germany

Moritz P. Reiter
School of Physics and Astronomy, University of Edinburgh, Edinburgh EH9 3FD, Scotland

Anna A. Kwiatkowski
University of Victoria, Victoria, British Columbia V8P 5C2, Canada

E-mail: tmurboeck@triumf.ca, aak@uvic.ca

Abstract While the nuclear deformation in the region around $Z = 40$ and $N = 60$ has been studied in great detail, the possible onset of nuclear deformation in the isotopic chain of krypton ($Z = 36$) is still a subject of controversy. Here, we present a high-precision mass measurement of the neutron-rich nuclide ^{96}Kr, as measured by the Multiple-Reflection Time-of-Flight Mass Spectrometer (MR-TOF-MS) at TRIUMF's Ion Trap for Atomic and Nuclear Science (TITAN). A statistical method, based on a hyper-exponentially modified Gaussian, has been employed to model the data. As such, the uncertainty introduced by overlapping peaks from beam contaminants was reduced and the mass excess of ^{96}Kr determined to be -53 097(57) keV. The capability of the method has been confirmed with measurements of the stable isotopic pair ^{40}Ar / ^{40}Ca, in which a relative accuracy $\Delta m/m$ of $3.5 \cdot 10^{-8}$ and a mass resolving power of more than 400 000 were achieved.

Keywords Atomic masses, Binding energy, Exotic nuclei, Time-of-flight mass spectrometer, Multiple reflection, hyper-exponentially modified Gaussian, HEMG

1 Introduction

High-precision mass spectrometry, providing direct information on the nuclear binding energy, has grown over the previous years to become a pivotal tool in nuclear physics. By revealing trends in the two-neutron separation energy, for instance, it facilitates the study of nuclear features such as magic numbers, midshell effects, and nuclear deformation [1].

The region of the nuclear chart around mass number $A = 100$, between the isotopic chains of krypton ($Z = 36$) and molybdenum ($Z = 42$), exhibits at $N = 60$ a remarkable change of shape. Since its discovery [2], considerable efforts have been made to understand the properties of the nuclides in this region [3,4,5,6,7]. In the krypton isotopic chain, the potential low-Z border of this region, charge radii [8] and excitation energies of low-lying states [9,10] suggest there is no sudden onset of deformation at $N = 60$. Rather, data indicate a smooth shape evolution between $N = 60$ and $N = 64$. This observation is in agreement with theoretical predictions, which suggest a transition from weakly to strongly deformed shapes around $N = 62, 63$ [11,12]. Indeed, ground-state binding energies of $^{94-97}$Kr ($N = 58 - 61$) provide no evidence of a shape transition [13,14]. Thus, high-precision mass spectrometry of the nuclei $^{98-100}$Kr is required to clarify if the krypton chain is the critical boundary of the $A = 100$ region of deformation.

To approach these neutron-rich nuclei, multiple-reflection time-of-flight mass spectrometry of ^{96}Kr has been performed. In the analysis of the data, peak shapes in the spectra were modeled with hyper-exponentially modified Gaussians (HEMG) [15], which helped to significantly reduce the uncertainty caused by contaminants in the radioactive ion beam.

2 Experimental Description

The experiment has been performed at TRIUMF's Ion Trap for Atomic and Nuclear science (TITAN) [16,17] located at TRIUMF's Isotope Separator and ACcelerator (ISAC) facility in Vancouver, Canada [18]. Radioactive nuclides for this ex-

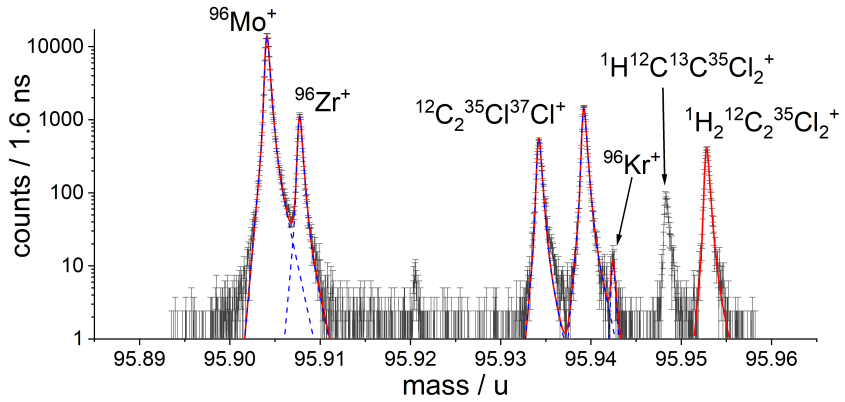

Fig. 1 Sample of the MR-TOF mass spectrum for mass 96 u. Prominent features besides $^{96}Kr^{+}$ are the doublet of $^{96}Mo^{+}$ and $^{96}Zr^{+}$, which has been used as a mass calibrant, and the molecule $^{1}H_2\,^{12}C_2\,^{35}Cl_2^{+}$, which has been used as a peak-shape calibrant for the HEMG distribution H_{22}.

periment have been produced by a primary 480 MeV proton beam of 10 μA impinging on a UC_x target. The reaction products diffused out of the target and through a water-cooled transfer line, impeding the diffusion of less volatile species, before being ionized by a Forced Electron Beam Induced Arc Discharge (FEBIAD) ion source [19]. The continuous radioactive ion beam (RIB) was transferred through a dipole magnet mass separator with a mass resolving power of approximately 2000 to reduce the beam to a single A/Q. The beam was then transported with an energy of 20 keV to the TITAN experiment, where it was trapped and cooled in a He-gas-filled radio-frequency quadrupole (RFQ) cooler-buncher [20]. Bunches of cooled ions were subsequently distributed to the MR-TOF-MS. The cycle time of 10 ms used in this experiment allowed for a maximum resolving power $R = m/\Delta m$ of about 200 000. The design of the TITAN MR-TOF-MS has been described in Ref. [21, 22] and a more detailed description of the system can be found in Ref. [23, 24].

3 Method of Data Analysis and Results

While the cold transfer line effectively impeded the diffusion of less volatile radioactive isotopes, the delivered beam still contained stable contaminant molecules formed in the FEBIAD ion source from residual gas. Next to the signal of $^{96}Kr^{+}$, two close-by molecular contaminants were observed with much higher intensities, whose long-range tails partially overlap with the ion of interest (IoI) peak (Fig. 1). Hence, for an accurate determination of the mass of ^{96}Kr, the data peak had to be fitted with a model that was capable of describing the non-Gaussian tails of these peaks.

An established statistical method for MR-TOF-MS peak-shape modeling beyond the simplistic Gaussian approach is the hyper-exponentially modified Gaussian (HEMG). Following the description in Ref. [15], a HEMG distribution H_{nm}

was defined by the convolution of a Gaussian with n left-hand sided and m right-handed sided exponential functions. The free parameters of the distribution are the center and width of the Gaussian, the decay constants and weights of the exponential functions, and the total area of the distribution. In a first step, the parameters of H_{nm} are determined using the method of least squares in a fit of a selected peak, the so-called peak-shape calibrant. In this case, the molecule $^{1}H_2\,^{12}C_2\,^{35}Cl_2{}^{+}$ has been chosen for this purpose because it has sufficiently high statistics and almost no overlap with other peaks. This step of fitting the molecule peak was repeated using various combinations of integer values for n and m. Of the tested distributions, a HEMG model H_{22} with $n = m = 2$ yielded the lowest reduced χ-squared of $\chi = 1.02$.

Since all isobaric species in a MR-TOF spectrum experience the same electric field, they share common peak features. In a second step, the obtained H_{22} from the $^{1}H_2\,^{12}C_2\,^{35}Cl_2{}^{+}$ peak can serve as a fitting model for any other data peak in the spectrum. For the remaining data, only the center position and the area of H_{22} were used as free parameters, while all other parameters were held constant. In this way, the group containing $^{96}Mo^{+}$ and $^{96}Zr^{+}$ and the group consisting of the IoI and two other molecules were fitted to determine the mass of $^{96}Kr^{+}$. The resulting reduced χ-squared of the fits for the doublet peak and the triplet peak were 6.85 and 1.88, respectively. The reduction of the goodness of fit when compared to that of the peak shape calibrant could be contributed to the significantly higher statistics of these peaks. This resulted in the emergence of peak-shape features not present in the original peak-shape calibrant and consequently not reflected by the applied H_{22} model.

The mass excess of ^{96}Kr was determined to be -53 097(57) keV, which is in excellent agreement with the previously reported value of -53 080(20) keV [14]. The total error budget was dominated by three contributions: the peak-shape uncertainty of the fitting model, the systematic uncertainty of the MR-TOF-MS, and the statistical uncertainty. For the peak-shape uncertainty, each fit parameter was individually varied by its uncertainty, while the other parameters were kept unchanged [25]. Subsequently, the peak center deviations of all parameters were quadratically added. This procedure was performed for both $^{96}Kr^{+}$ and the mass calibrant, $^{96}Mo^{+}$, to yield a total peak-shape uncertainty of 48 keV. The systematic uncertainty of the MR-TOF mass spectrometer had been accounted for with a relative uncertainty of $\Delta m/m = 3.0 \cdot 10^{-7}$ [26], which amounts to 27 keV. A typical statistical uncertainty for a HEMG distribution with full width at half maximum (FWHM) and number of counts N_{counts} [25] is given by

$$\sigma_{\mathrm{stat}} = A_{\mathrm{stat}} \frac{\mathrm{FWHM}}{\sqrt{N_{\mathrm{counts}}}} \approx 0.53 \frac{\mathrm{FWHM}}{\sqrt{N_{\mathrm{counts}}}}. \quad (1)$$

In this case the statistical uncertainty amounted to 15 keV. Since this was only a minor contribution to the total error budget, possible deviations of A_{stat} from the value given in Ref. [25], which could be caused by the specifics of the peak shape, were not considered.

The peak-shape uncertainty was the single largest contribution to the error budget, and its influence on the fitting model was further investigated. In particular, due to the large amount of contaminants in the spectrum, it was not possible to select a peak-shape calibrant without impairment from neighboring peaks. As a consequence, the domain over which the model was fitted to the peak-shape

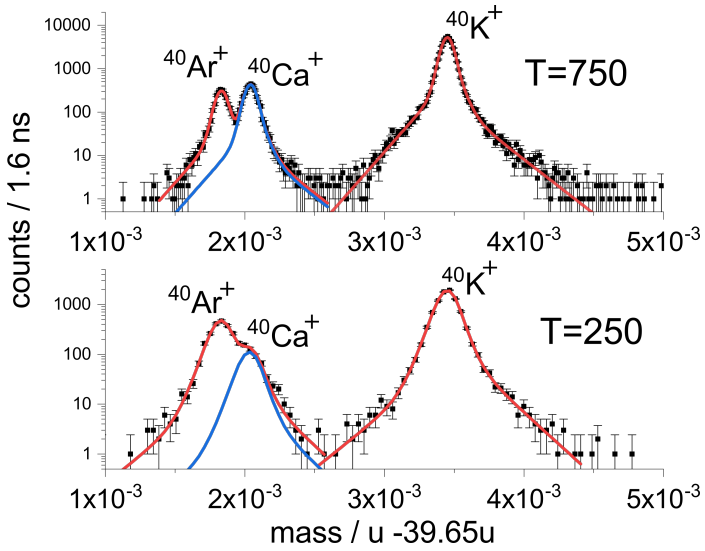

Fig. 2 A spectrum of three isobaric species ^{40}Ar$^+$, ^{40}Ca$^+$, and ^{40}K$^+$ recorded with 750 isochronous turns T (top panel) and 250 isochronous turns (bottom panel), respectively. The relative intensities in the Ar-Ca doublet are 1:1.4 and 1:0.24 in the top and bottom panel, respectively.

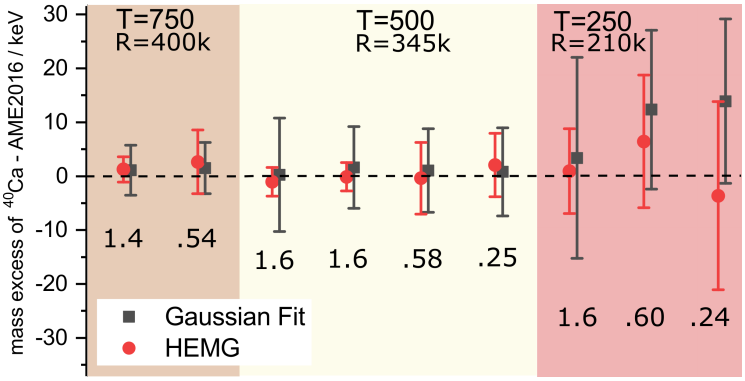

Fig. 3 The deviation of the measured ^{40}Ca mass excess from the AME2016 value. The number below each data point indicates the intensity of ^{40}Ca$^+$ relative to ^{40}Ar$^+$. T describes the number of isochronous turns and R the mass resolving power. See the text for more details.

calibrant affected the obtained parameters of the distribution H_{22} and in turn the ^{96}Kr mass value and its uncertainty. However, by systematically changing the domain and comparing the mass values obtained from different distributions, it proved that the relative uncertainty $\Delta m/m$ introduced by this arbitrary choice was only $2 \cdot 10^{-8}$, which stresses the robustness of the approach.

In order to further investigate the HEMG peak-shape uncertainty in a well-controlled test-case, masses obtained for three isobaric species, ^{40}Ar$^+$, ^{40}Ca$^+$, and ^{40}K$^+$ were compared when either a HEMG model or a conventional Gaussian was used (Fig. 2). Both K and Ca ions were produced by a thermal ion source, while

argon ions were independently created from residual Ar in the MR-TOF-MS beam-preparation region. This permitted a controllable intensity of $^{40}Ca^{+}$ while keeping the amount of $^{40}Ar^{+}$ approximately constant. Furthermore, the peak separation within the doublet was varied by selecting different isochronous turn numbers, and consequently different mass resolving powers. Three isochronous turn numbers, 250, 500, and 750, were used with resolving powers ranging between 200 000 and 400 000, which corresponded to a peak separation of 1 and 2 FWHM, respectively. With $^{40}Ar^{+}$ as a mass calibrant, the mass of $^{40}Ca^{+}$ was determined from either a H_{22} model or the Gaussian fit. The deviation from the mass value reported in the Atomic Mass Evaluation 2016 (AME2016) is shown in Fig. 3, with error bars displaying the combined peak-shape and statistical uncertainty. In general, the uncertainties obtained from the HEMG model are comparable or significantly smaller than those from the Gaussian model. That was especially true for the measurements with 250 isochronous turns, where peaks overlapped more due to the lower resolving power. The ^{40}Ca mass excess, determined from the weighted average of the individual HEMG results, was found to be -34 846.0 keV with an uncertainty of 1.3 keV, which is equivalent to a 0.4 keV deviation from the AME2016. The excellent agreement with AME16 demonstrates the accuracy of the HEMG method to determine the centroid of overlapping peaks and therefore the mass.

4 Summary and Outlook

In this publication, we present the high-precision mass measurement of ^{96}Kr, fitting MR-TOF-MS spectra with a statistical method using HEMG distributions. Despite a spectrum rich in contaminant species, this approach allowed a total uncertainty of 57 keV and a relative uncertainty of $6.4 \cdot 10^{-7}$, respectively. The validity of the employed method was confirmed in a measurement of the three isobaric species ^{40}Ar, ^{40}Ca, and ^{40}K to a relative uncertainty of $3.5 \cdot 10^{-8}$. The HEMG method is requisite in MR-TOF-MS spectra with overlapping peaks, common for highly contaminated beams. Such is our expectation for beams produced at ISOL facilities with a FEBIAD ion source. If the contamination is not overwhelming relative to the ion of interest, these measurements allow us to pursue heavier neutron-rich krypton isotopes to probe the possible onset of nuclear deformation.

Acknowledgements This work was supported by BMBF (grants 05P15RGFN1 and 05P12RGFN8), and by the JLU and GSI under the JLU-GSI strategic Helmholtz partnership agreement, by the Canada-UK foundation, and by France's IN2P3 and the Programme Internationale de Coopération Scientifique "PACIFIC". E. L. acknowledges support from Brazil's Conselho Nacional de Desenvolvimento Cientifico e Tecnolgico (CNPq) under Science Without Borders' grant no. 249121/2013-1.

References

1. Blaum, K., Dilling, J., Nörtershäuser, W.: Precision atomic physics techniques for nuclear physics with radioactive beams. Physica Scripta **T152**, 014,017 (2013). DOI 10.1088/0031-8949/2013/t152/014017. URL `https://doi.org/10.1088%2F0031-8949%2F2013%2Ft152%2F014017`

2. Johansson, S.A.: Gamma de-excitation of fission fragments: (ii). delayed radiation. Nuclear Physics **64**(1), 147 – 160 (1965). DOI https://doi.org/10.1016/0029-5582(65)90847-3. URL http://www.sciencedirect.com/science/article/pii/0029558265908473
3. Cheifetz, E., Jared, R.C., Thompson, S.G., Wilhelmy, J.B.: Experimental information concerning deformation of neutron rich nuclei in the $A \sim 100$ region. Phys. Rev. Lett. **25**, 38–43 (1970). DOI 10.1103/PhysRevLett.25.38. URL https://link.aps.org/doi/10.1103/PhysRevLett.25.38
4. Azuma, R., Borchert, G., Carraz, L., Hansen, P., Jonson, B., Mattsson, S., Nielsen, O., Nyman, G., Ragnarsson, I., Ravn, H.: The strongly deformed nucleus 100Sr. Physics Letters B **86**(1), 5 – 8 (1979). DOI https://doi.org/10.1016/0370-2693(79)90607-5. URL http://www.sciencedirect.com/science/article/pii/0370269379906075
5. Kirchuk, E., Federman, P., Pittel, S.: Nuclear deformation in the mass-80 and mass-100 regions. Phys. Rev. C **47**, 567–572 (1993). DOI 10.1103/PhysRevC.47.567. URL https://link.aps.org/doi/10.1103/PhysRevC.47.567
6. Hotchkis, M., Durell, J., Fitzgerald, J., Mowbray, A., Phillips, W., Ahmad, I., Carpenter, M., Janssens, R., Khoo, T., Moore, E., Morss, L., Benet, P., Ye, D.: Rotational bands in the mass 100 region. Nuclear Physics A **530**(1), 111 – 134 (1991). DOI https://doi.org/10.1016/0375-9474(91)90758-X. URL http://www.sciencedirect.com/science/article/pii/037594749190758X
7. Smith, A.G., Durell, J.L., Phillips, W.R., Urban, W., Sarriguren, P., Ahmad, I.: Lifetime measurements and nuclear deformation in the $A \approx 100$ region. Phys. Rev. C **86**, 014,321 (2012). DOI 10.1103/PhysRevC.86.014321. URL https://link.aps.org/doi/10.1103/PhysRevC.86.014321
8. Keim, M., Arnold, E., Borchers, W., Georg, U., Klein, A., Neugart, R., Vermeeren, L., Silverans, R., Lievens, P.: Laser-spectroscopy measurements of 72-96Kr spins, moments and charge radii. Nuclear Physics A **586**(2), 219 – 239 (1995). DOI https://doi.org/10.1016/0375-9474(94)00786-M. URL http://www.sciencedirect.com/science/article/pii/037594749400786M
9. Albers, M., Warr, N., Nomura, K., Blazhev, A., Jolie, J., Mücher, D., Bastin, B., Bauer, C., Bernards, C., Bettermann, L., Bildstein, V., Butterworth, J., Cappellazzo, M., Cederkäll, J., Cline, D., Darby, I., Das Gupta, S., Daugas, J.M., Davinson, T., De Witte, H., Diriken, J., Filipescu, D., Fiori, E., Fransen, C., Gaffney, L.P., Georgiev, G., Gernhäuser, R., Hackstein, M., Heinze, S., Hess, H., Huyse, M., Jenkins, D., Konki, J., Kowalczyk, M., Kröll, T., Krücken, R., Litzinger, J., Lutter, R., Marginean, N., Mihai, C., Moschner, K., Napiorkowski, P., Nara Singh, B.S., Nowak, K., Otsuka, T., Pakarinen, J., Pfeiffer, M., Radeck, D., Reiter, P., Rigby, S., Robledo, L.M., Rodríguez-Guzmán, R., Rudigier, M., Sarriguren, P., Scheck, M., Seidlitz, M., Siebeck, B., Simpson, G., Thöle, P., Thomas, T., Van de Walle, J., Van Duppen, P., Vermeulen, M., Voulot, D., Wadsworth, R., Wenander, F., Wimmer, K., Zell, K.O., Zielinska, M.: Evidence for a smooth onset of deformation in the neutron-rich Kr isotopes. Phys. Rev. Lett. **108**, 062,701 (2012). DOI 10.1103/PhysRevLett.108.062701. URL https://link.aps.org/doi/10.1103/PhysRevLett.108.062701
10. Flavigny, F., Doornenbal, P., Obertelli, A., Delaroche, J.P., Girod, M., Libert, J., Rodriguez, T.R., Authelet, G., Baba, H., Calvet, D., Château, F., Chen, S., Corsi, A., Delbart, A., Gheller, J.M., Giganon, A., Gillibert, A., Lapoux, V., Motobayashi, T., Nikura, M., Paul, N., Roussé, J.Y., Sakurai, H., Santamaria, C., Steppenbeck, D., Taniuchi, R., Uesaka, T., Ando, T., Arici, T., Blazhev, A., Browne, F., Bruce, A., Carroll, R., Chung, L.X., Cortés, M.L., Dewald, M., Ding, B., Franchoo, S., Górska, M., Gottardo, A., Jungclaus, A., Lee, J., Lettmann, M., Linh, B.D., Liu, J., Liu, Z., Lizarazo, C., Momiyama, S., Moschner, K., Nagamine, S., Nakatsuka, N., Nita, C., Nobs, C.R., Olivier, L., Orlandi, R., Patel, Z., Podolyák, Z., Rudigier, M., Saito, T., Shand, C., Söderström, P.A., Stefan, I., Vaquero, V., Werner, V., Wimmer, K., Xu, Z.: Shape evolution in neutron-rich krypton isotopes beyond $N = 60$: First spectroscopy of ^{98,100}Kr. Phys. Rev. Lett. **118**, 242,501 (2017). DOI 10.1103/PhysRevLett.118.242501. URL https://link.aps.org/doi/10.1103/PhysRevLett.118.242501
11. Manea, V., Atanasov, D., Beck, D., Blaum, K., Borgmann, C., Cakirli, R.B., Eronen, T., George, S., Herfurth, F., Herlert, A., Kowalska, M., Kreim, S., Litvinov, Y.A., Lunney, D., Neidherr, D., Rosenbusch, M., Schweikhard, L., Wienholtz, F., Wolf, R.N., Zuber, K.: Collective degrees of freedom of neutron-rich $A \approx 100$ nuclei and the first mass measurement of the short-lived nuclide ^{100}rb. Phys. Rev. C **88**, 054,322 (2013). DOI 10.1103/PhysRevC.88.054322. URL https://link.aps.org/doi/10.1103/PhysRevC.88.054322

12. de Roubin, A., Atanasov, D., Blaum, K., George, S., Herfurth, F., Kisler, D., Kowalska, M., Kreim, S., Lunney, D., Manea, V., Minaya Ramirez, E., Mougeot, M., Neidherr, D., Rosenbusch, M., Schweikhard, L., Welker, A., Wienholtz, F., Wolf, R.N., Zuber, K.: Nuclear deformation in the $A \approx 100$ region: Comparison between new masses and mean-field predictions. Phys. Rev. C **96**, 014,310 (2017). DOI 10.1103/PhysRevC.96.014310. URL https://link.aps.org/doi/10.1103/PhysRevC.96.014310
13. Delahaye, P., Audi, G., Blaum, K., Carrel, F., George, S., Herfurth, F., Herlert, A., Kellerbauer, A., Kluge, H.J., Lunney, D., Schweikhard, L., Yazidjian, C.: High-accuracy mass measurements of neutron-rich Kr isotopes. Phys. Rev. C **74**, 034,331 (2006). DOI 10.1103/PhysRevC.74.034331. URL https://link.aps.org/doi/10.1103/PhysRevC.74.034331
14. Naimi, S., Audi, G., Beck, D., Blaum, K., Böhm, C., Borgmann, C., Breitenfeldt, M., George, S., Herfurth, F., Herlert, A., Kowalska, M., Kreim, S., Lunney, D., Neidherr, D., Rosenbusch, M., Schwarz, S., Schweikhard, L., Zuber, K.: Critical-point boundary for the nuclear quantum phase transition near $A = 100$ from mass measurements of ^{96,97}Kr. Phys. Rev. Lett. **105**, 032,502 (2010). DOI 10.1103/PhysRevLett.105.032502. URL https://link.aps.org/doi/10.1103/PhysRevLett.105.032502
15. Purushothaman, S., Andrés, S.A.S., Bergmann, J., Dickel, T., Ebert, J., Geissel, H., Hornung, C., Plaß, W., Rappold, C., Scheidenberger, C., Tanaka, Y., Yavor, M.: Hyperemg: A new probability distribution function composed of exponentially modified gaussian distributions to analyze asymmetric peak shapes in high-resolution time-of-flight mass spectrometry. International Journal of Mass Spectrometry **421**, 245 – 254 (2017). DOI https://doi.org/10.1016/j.ijms.2017.07.014. URL http://www.sciencedirect.com/science/article/pii/S1387380616302913
16. Dilling, J., Bricault, P., Smith, M., Kluge, H.J.: The proposed titan facility at isac for very precise mass measurements on highly charged short-lived isotopes. Nuclear Instruments and Methods in Physics Research Section B: Beam Interactions with Materials and Atoms **204**, 492 – 496 (2003). DOI https://doi.org/10.1016/S0168-583X(02)02118-3. URL http://www.sciencedirect.com/science/article/pii/S0168583X02021183. 14th International Conference on Electromagnetic Isotope Separators and Techniques Related to their Applications
17. Dilling, J., Baartman, R., Bricault, P., Brodeur, M., Blomeley, L., Buchinger, F., Crawford, J., López-Urrutia, J.C., Delheij, P., Froese, M., Gwinner, G., Ke, Z., Lee, J., Moore, R., Ryjkov, V., Sikler, G., Smith, M., Ullrich, J., Vaz, J.: Mass measurements on highly charged radioactive ions, a new approach to high precision with TITAN. International Journal of Mass Spectrometry **251**(2), 198 – 203 (2006). DOI https://doi.org/10.1016/j.ijms.2006.01.044. URL http://www.sciencedirect.com/science/article/pii/S1387380606000777. ULTRA-ACCURATE MASS SPECTROMETRY AND RELATED TOPICS Dedicated to H.-J. Kluge on the occasion of his 65th birthday anniversary
18. Ball, G.C., Hackman, G., Krücken, R.: The TRIUMF-ISAC facility: two decades of discovery with rare isotope beams. Physica Scripta **91**(9), 093,002 (2016). DOI 10.1088/0031-8949/91/9/093002. URL https://doi.org/10.1088%2F0031-8949%2F91%2F9%2F093002
19. Schultz, B.E., Sandor, J., Kunz, P., Mjøs, A., Kester, O., Ame, F.: FEBIAD ion source development at TRIUMF-ISAC. in: 9th International Particle Accelerator Conference (IPAC 2018), Vancouver, Canada, 2018, p. THPML041. DOI 10.18429/JACoWIPAC2018-THPML041
20. Brunner, T., Smith, M., Brodeur, M., Ettenauer, S., Gallant, A., Simon, V., Chaudhuri, A., Lapierre, A., Mané, E., Ringle, R., Simon, M., Vaz, J., Delheij, P., Good, M., Pearson, M., Dilling, J.: TITAN's digital RFQ ion beam cooler and buncher, operation and performance. Nuclear Instruments and Methods in Physics Research Section A: Accelerators, Spectrometers, Detectors and Associated Equipment **676**, 32 – 43 (2012). DOI https://doi.org/10.1016/j.nima.2012.02.004. URL http://www.sciencedirect.com/science/article/pii/S0168900212001398
21. Plaß, W.R., Dickel, T., Czok, U., Geissel, H., Petrick, M., Reinheimer, K., Scheidenberger, C., I.Yavor, M.: Isobar separation by time-of-flight mass spectrometry for low-energy radioactive ion beam facilities. Nuclear Instruments and Methods in Physics Research Section B: Beam Interactions with Materials and Atoms **266**(19), 4560 – 4564 (2008). DOI https://doi.org/10.1016/j.nimb.2008.05.079. URL http://www.sciencedirect.com/science/article/pii/S0168583X08007763. Proceedings of the XVth International Conference on Electromagnetic Isotope Separators and Techniques Related to their Applications

22. Dickel, T., Plaß, W., Becker, A., Czok, U., Geissel, H., Haettner, E., Jesch, C., Kinsel, W., Petrick, M., Scheidenberger, C., Simon, A., Yavor, M.: A high-performance multiple-reflection time-of-flight mass spectrometer and isobar separator for the research with exotic nuclei. Nuclear Instruments and Methods in Physics Research Section A: Accelerators, Spectrometers, Detectors and Associated Equipment **777**, 172 – 188 (2015). DOI https://doi.org/10.1016/j.nima.2014.12.094. URL http://www.sciencedirect.com/science/article/pii/S0168900214015629
23. Jesch, C., Dickel, T., Plaß, W.R., Short, D., Andres, S.A.S., Dilling, J., Geissel, H., Greiner, F., Lang, J., Leach, K.G., Lippert, W., Scheidenberger, C., Yavor, M.I.: The MR-TOF-MS isobar separator for the TITAN facility at TRIUMF. In: M. Wada, P. Schury, Y. Ichikawa (eds.) TCP 2014, pp. 175–184. Springer International Publishing, Cham (2017)
24. Dickel, T., San Andrés, S.A., Beck, S., Bergmann, J., Dilling, J., Greiner, F., Hornung, C., Jacobs, A., Kripko-Koncz, G., Kwiatkowski, A., Leistenschneider, E., Pikthtelev, A., Plaß, W.R., Reiter, M.P., Scheidenberger, C., Will, C., for the TITAN collaboration: Recent upgrades of the multiple-reflection time-of-flight mass spectrometer at TITAN, TRIUMF. Hyperfine Interactions **240**(1), 62 (2019). DOI 10.1007/s10751-019-1610-y. URL https://doi.org/10.1007/s10751-019-1610-y
25. Ayet San Andrés, S., Hornung, C., Ebert, J., Plaß, W.R., Dickel, T., Geissel, H., Scheidenberger, C., Bergmann, J., Greiner, F., Haettner, E., Jesch, C., Lippert, W., Mardor, I., Miskun, I., Patyk, Z., Pietri, S., Pihktelev, A., Purushothaman, S., Reiter, M.P., Rink, A.K., Weick, H., Yavor, M.I., Bagchi, S., Charviakova, V., Constantin, P., Diwisch, M., Finlay, A., Kaur, S., Knöbel, R., Lang, J., Mei, B., Moore, I.D., Otto, J.H., Pohjalainen, I., Prochazka, A., Rappold, C., Takechi, M., Tanaka, Y.K., Winfield, J.S., Xu, X.: High-resolution, accurate multiple-reflection time-of-flight mass spectrometry for short-lived, exotic nuclei of a few events in their ground and low-lying isomeric states. Phys. Rev. C **99**, 064,313 (2019). DOI 10.1103/PhysRevC.99.064313. URL https://link.aps.org/doi/10.1103/PhysRevC.99.064313
26. Will, C.: Time-of-flight mass spectrometer and isobar separator - characterization and first experiments (2017)